WFPS-TME-80-014
OCTOBER 1980
UC-21

CONF-801011--77

THE WESTINGHOUSE ICF POWER PLANT STUDY

E. W. SUCOV, ET. AL.

MASTER

This paper was submitted to the
Proceedings of the 4th ANS
Topical Meeting on the Technology
of Controlled Nuclear Fusion,
King of Prussia, PA
October 14-17, 1980

fusion power systems department

Westinghouse Electric Corporation
P.O. Box 10864, Pgh. Pa. 15236

DISCLAIMER

Printed in the United States of America
Available from
National Technical Information Service
U.S. Department of Commerce
5285 Port Royal Road
Springfield, VA 22161

NTIS price codes
Printed copy:_____
Microfiche copy: A01

THE WESTINGHOUSE ICF POWER PLANT DESIGN STUDY

E.W. Sucov, J.S. Karbowski, T.V. Prevenslik, L. Green,
A.Y. Lee, R.E. Gold, H.J. Garber, M. Sniderman, R.V. Babcock,
M.D. Nahemow, L.H. Taylor, J.R. Easoz, W.C. Brenner,
D.A. Sink, E.M. Iwinski, R.J. Ravas

Westinghouse Electric Corporation
Fusion Power Systems Department
Pittsburgh PA 15236

In this study, two different electric power plants for the production of about 1000 MWe which were based on a CO_2 laser driver and on a heavy ion driver have been developed and analyzed. The purposes of this study were: (1) to examine in a self consistent way the technological and institutional problems that need to be confronted and solved in order to produce commercially competitive electricity in the 2020 time frame from an inertial fusion reactor, and (2) to compare, on a common basis, the consequences of using two different drivers to initiate the DT fuel pellet explosions. Analytic descriptions of size/performance/cost relationships for each of the subsystems comprising the power plant (see Figure 1) have been combined into an overall computer code which models the entire plant. This overall model has been used to conduct trade studies which examine the consequences of varying critical design values around the reference point.

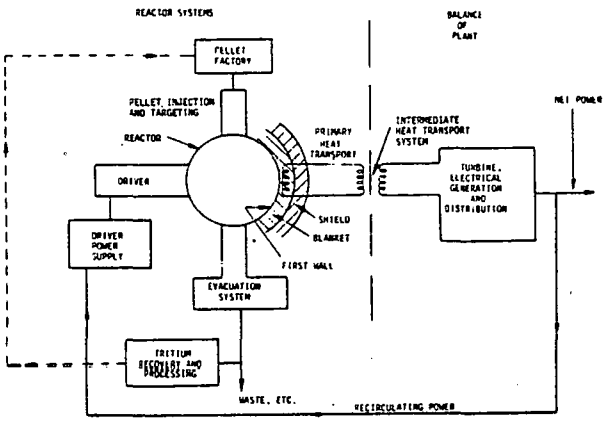

Figure 1. Functional Schematic of an Inertial Confinement Fusion Power Plant

TABLE 1
ICF ELECTRIC GENERATING PLANT SYSTEM PARAMETERS

	Laser	Heavy Ion
Pellet Thermal Power	3500 MWt	3500 MWt
Driver Energy	2 MJ	2 MJ
Pellet Gain, Q	175	175
Driver Efficiency, η	10%	30%
ηQ	17.5	52.5
Pellet Yield	350 MJ	350 MJ
Rep Rate	10 Hz	10 Hz
Driver Power	200 MWe	67 MWe
Total Blanket Thermal Power	4300 MWt	4300 MWt
Gross Electric Power	1565 MWe	1565 MWe
Net Electric Power	1207 MWe	1346 MWe
Thermal to Net Electric Conversion Efficiency	28.1%	31.3%
Recirculating Fraction	22.9%	14.0%
Cavity Gas Pressure	10^{-1} torr	5×10^{-4} torr
Cavity Radius	10 m	10 m
Cavity Shape	Spherical	Spherical
First Wall Configuration	Tubular	Tubular
First Wall Material	HT-9 Steel	HT-9 Steel
First Wall Protective Coating	Ta	Ta
Coolant/Blanket	Liquid Lithium	Liquid Lithium
Tritium Breeding Ratio	>1.2	>1.2

Reactor Design

Our design irradiates the pellet from two opposite sides by using drivers which deliver 2 MJ to the pellet at a repetition rate of 10 Hz. The pellets have a gain of 175 and a yield of 350 MJ per shot. Because the laser efficiency at 10% is much lower than the 30% efficiency of heavy ion beams, the net electric power available from the laser plant is about 140 MW less than that from a heavy ion plant. The features of our reactor design are summarized in Table 1; the power flow through the two plants is shown in Figures 2 and 3.

The essential engineering problem to be solved in an ICF reaction chamber is to design a first wall which can carry away the steady state average surface heat and at the same time survive the transient temperature increase generated by x-rays and ions from the pellet explosion. Conditions for transmission of the laser beam and the ion beam to the target require cavity pressure to be $<10^{-1}$ torr and $<5 \times 10^{-4}$ torr respectively. These pressures were chosen as reference points in our design. While the presence of 10^{-1} torr background gas in the laser cavity does offer some protection to the first wall against low

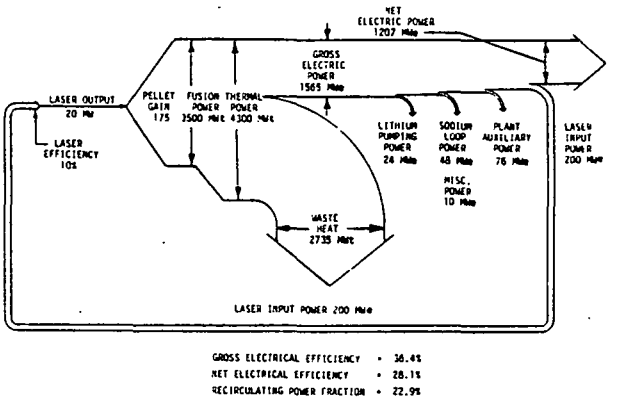

Figure 2. Power Flow Diagram for the Reference Laser Fusion Reactor

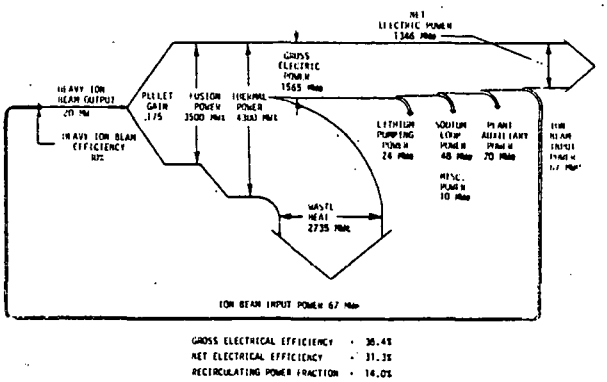

Figure 3. Power Flow Diagram for the Reference Heavy Ion Beam Fusion Reactor

energy x-rays and ions, it is not effective against the high energy x-rays and ions expected from high gain pellets. Thus, our design for the first wall is the same for both the laser and the ion beam drivers.

Our solution to the problem of removing the steady state heat load takes advantage of the fact that the x-rays and ions are absorbed in a thin ($\sim$1μm) surface layer of the wall while the neutrons must be absorbed in a thick ($\sim$1 m) blanket. Because the x-rays and ions contain 45% of the fusion power and are absorbed on the surface of the wall, the surface heat flux is about 1.3 MW/m^2; this is removed by liquid lithium flowing through thin walled steel tubes with a maximum velocity of 18 m/s. The neutrons, on the other hand, carry 55% of the power and are slightly absorbed in the first wall coolant and mainly absorbed in the volume of the 58 cm thick slowly flowing liquid lithium blanket situated behind the tubular first wall. A vacuum tight spherical cavity can be formed from tubes by bending a properly tapered tube in a semicircle as shown in Figure 4. The semicircular tubes, when placed side by side and welded, form a rippled spherical surface. The semicircle cannot be completed because it is necessary to provide an inlet and outlet for the flowing lithium. As a consequence, the sphere automatically has two large circular openings on the equatorial plane at either side of the sphere through which the beams can be injected and to which vacuum pumps can be connected. Because the thin shell tubes would buckle under the weight of the lithium blanket, a backing plate is introduced to take up this load. This arrangement is shown in Figure 5. Tritium breeding ratio for this configuration is about 1.22.

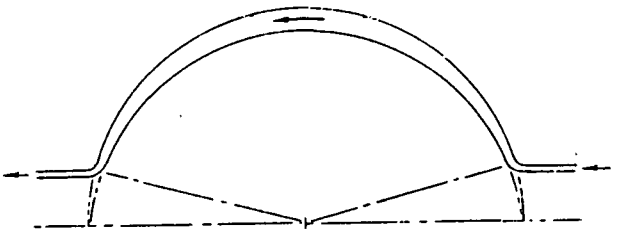

Figure 4. First Wall Coolant Tube Schematic

Our solution to the problem of dry first wall survival under transient temperature increases is to protect the first wall surface of the tubes (facing the explosion) with a metallic layer whose melting temperature is above the peak temperature transient caused by the x-rays. This coating is also required to buffer the steel tubes from the large temperature transients which might otherwise destroy them due to thermal stress cyclic fatigue. Examination of the interaction between pellet heavy metal debris and an undestroyed first wall showed that, no matter what the original first wall material was, the rate of condensible metal deposition on the first wall was so great that the first wall coating material must be considered to be the same as the pellet metal. The choice of heavy metal for the pellet therefore becomes a joint decision of the pellet designer and the reaction chamber designer. Candidate heavy metals currently being used in pellet designs were reviewed and Ta was selected because of its high melting temperature, ease of handling, high thermal conductivity and high strength. The viability of a Ta layer 1 mm thick was verified by computer calculations, including results from

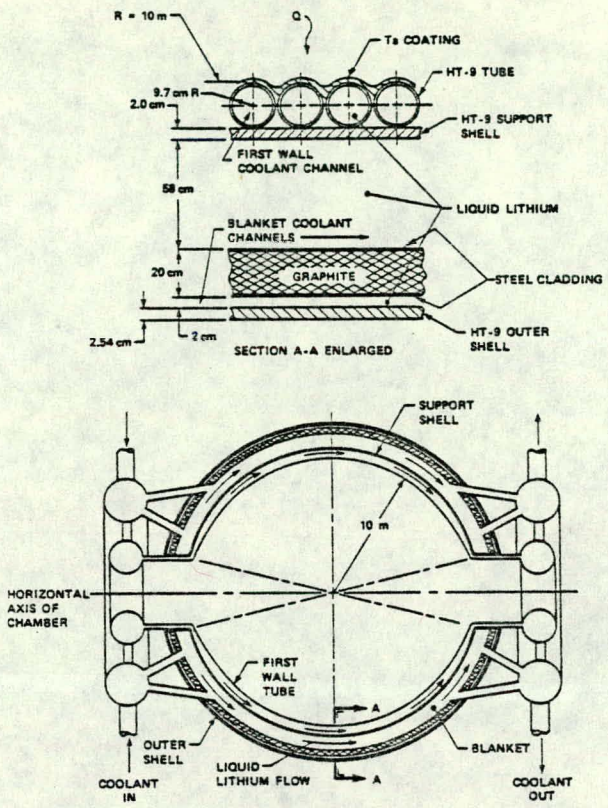

Figure 5. Schematic Representation of the Tubular First Wall and Blanket Concept.

the CHART D code, which showed that: (1) the temperature of the Ta surface was always below its melting point, (2) internal stresses were not sufficient to cause spallation of the Ta, and (3) the temperature increase at the Ta-steel interface was negligible.

Debris from the pellet explosions consists of non-condensible gases (H, D, T, He, O, CO_2, etc.) and the condensible Ta. The vacuum system is designed to pump out the excess gas created by each explosion in less than 100 ms; total required pumping speed is 10^5 ℓ/s for the heavy ion beam case. Condensibles deposit about 95% of their mass on the inner surface of the first wall after each shot and about 5% in the major ducts on either side of the reaction chamber. The Ta deposit adds to the Ta which coats the first wall; it is removed by intermittently vaporizing it and allowing 5% of this vapor to redeposit outside the chamber on the duct walls. Vaporization is achieved by inserting a pellet into the firing system at preprogrammed intervals whose x-ray yield would cause the Ta to melt and vaporize. Final removal of the Ta deposit in the vacuum ducts is incorporated in the regular maintenance schedule.

Driver Designs

The CO_2 laser delivers 2 MJ of 10.6 μm radiation to the pellet through a cavity pressure of 10^{-1} torr by combining 108 20 kJ beams arranged in 12 beam ducts (6 per side) carrying 9 beams per duct. The nine beams in a given duct are sequentially extracted from a Power Amplifier Module (PAM) over a total period of 1.2 μs in order to achieve the design goal of 10% driver efficiency. These beams are recombined by introducing appropriate mirrors in a laser/mirror hall which equalize optical path length to the target. Entry windows are made of salt (NaCl) which provides good transmission at 10.6 μm; however, salt windows are limited to peak fluxes of 3 J/cm^2 for ns pulses and the mechanical strength of flat salt windows limits their aperture to about 100 cm for a one atmosphere pressure differential. This defines the maximum energy per beam to be about 20 kJ. Diffraction laws applied to 10.6 μm radiation require the distance from the final mirror to a 1 mm pellet to be ∿30 m. Since the cavity radius is 10 m, the additional length allows the introduction of gas flowing from the final mirror to the cavity to act as a shield against pellet debris, particulate radiation and soft x-rays. To protect the environment against neutron radiation effects, the laser beams are brought from the entry window to the final mirror through four right angle turns in a labyrinth surrounded by shielding material. Additional protection against leaks or fractures of the NaCl windows is afforded by reducing the beam cross sections and passing all nine of them through a single 0.9 m diameter ball valve. These features are shown in Figure 6. The laser/cavity/containment building interface is shown in Figure 7.

The heavy ion beam driver accelerates bunches of singly charged Xe 131 ions through a sequence of low beta (v/c) Wideroe linacs up to 800 MeV followed by about 4 km of high beta Alvarez linacs to reach 10 GeV. Each beam goes into a storage ring of radius 113 m which accumulates and compresses the bunches to make 13 ns pulses containing 800A each. A total of four storage rings carrying five beams each generate the 2 MJ pulse. A schematic representation of the heavy ion beam accelerator and storage ring system is shown in Figure 8. To prevent neutrons from back streaming down the open accelerator tube, the ion beam is bent into the entry port by a 1.2 tesla bending magnet that is 9 meters long; the neutron energy is absorbed in neutron dumps shown in Figure 8. Cavity pressure is set at 5 x 10^{-4} torr to allow ballistic aiming and transport of the ion beam to the target. Since pressure in the stor-

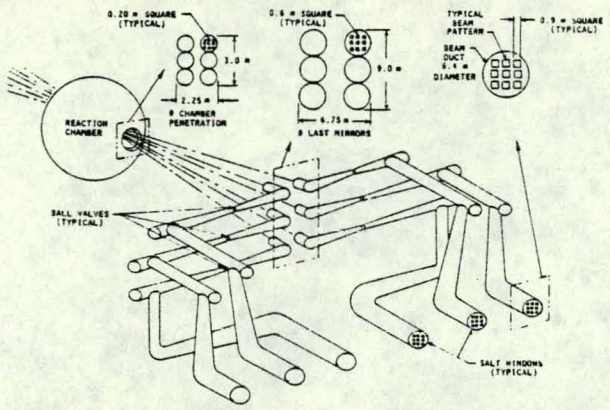

Figure 6. Laser Duct and Beam Concept Showing Duct Arrangement and Beam Pattern for 4-Bend Configuration.

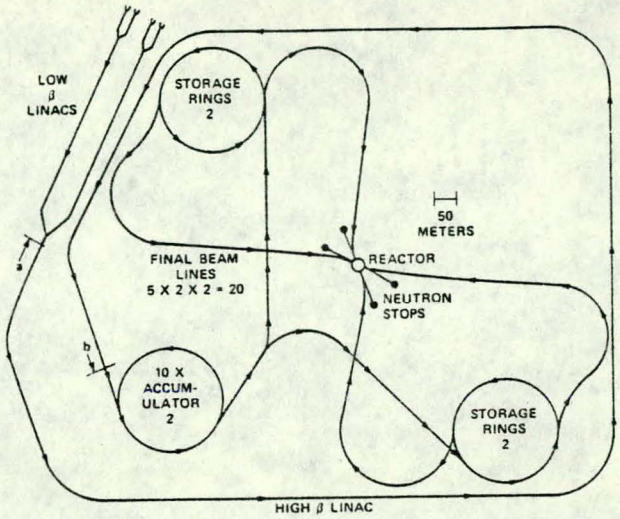

Figure 8. Schematic Representation of 10 GeV Xe^{+} Heavy Ion RF Linac Driver.

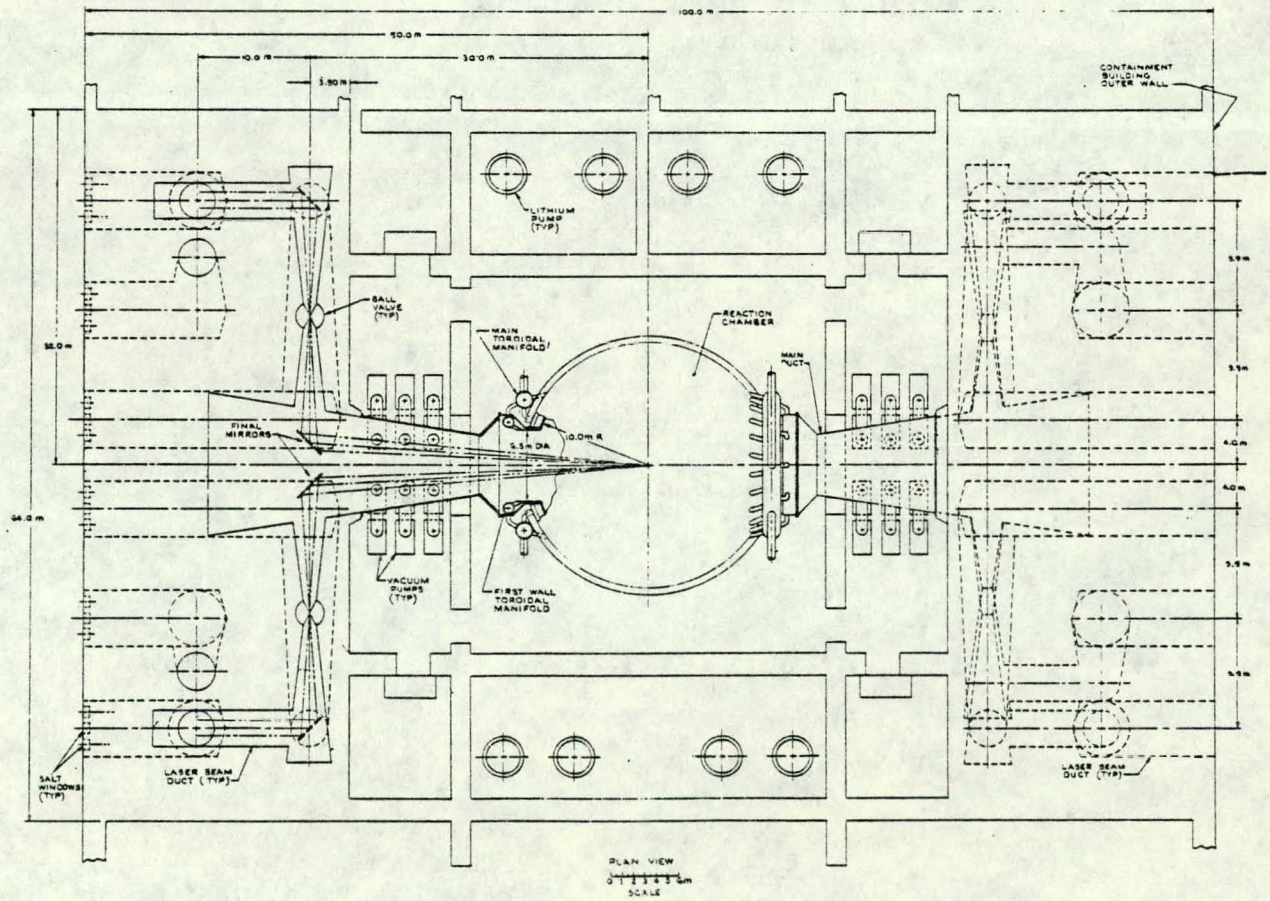

Figure 7. Plan View of the Reactor Building for the Laser Driver Concept

age rings is set at 10^{-10} torr to prevent excessive losses due to scattering during the 1 ms storage time, differential pumping is introduced over the distance between storage ring and cavity. The ion beam is focused to a radius of 2.5 mm at a distance of 15 m by two sets of quadrupole triplet magnets 40 m apart. Figure 9 shows how the ion beams enter the reaction chamber through their final triplet focusing magnets. The conical arrangement is required for ballistic aiming of the ion beams on the target area.

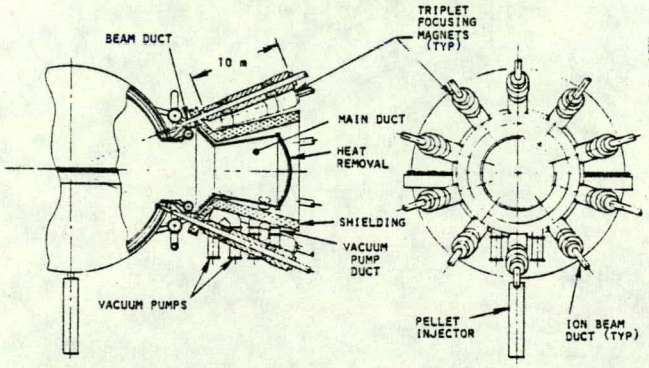

Figure 9. Reaction Chamber Interfaces Showing Relationship Between Focusing Magnets, Ion Beam Ducts and Vacuum Pumps

Pellet Fabrication and Injection

According to current understanding of pellet design, pellets capable of generating the required gain of 175 consist of an inner sphere containing the fuel and final tamper which is concentrically suspended inside an outer sphere containing the ablator and initial tamper. We have devised a novel method for suspending the inner sphere accurately and also maintaining the concentricity during injection into the reaction cavity. The essential concept is shown in Figure 10; it consists of an array of fibers in the two halves of the outer sphere which, when joined together, provide a confining nest for the inner sphere. These fibers would vaporize at the onset of implosion, and would produce a low pressure atmosphere between the outer and inner spheres and, more importantly, would remove high thermal conductivity paths from the outer to inner spheres which tend to destroy the spherical symmetry of the implosion.

Pellets must be injected with velocity greater than 100 m/s in order to traverse the 10 m to the target region in a time small compared to the interval between pulses. An injection system has been conceived which provides extremely accurate control over the pellet velocity and direction by utilizing a linear synchronous motor to accelerate a sabot which carries the pellet. The pellet is separated from the sabot by introducing a coil near the end of the acceleration track which decelerates the sabot; the pellet continues through a precision bore tube at the final velocity while the sabot is captured and returned. This scheme maintains pellet cryogenic temperatures, does not introduce gas into the cavity, is compatible with high speed, repeated operation and, because of the sabot separation concept, is expected to exhibit scatter of less than 100 μrad.

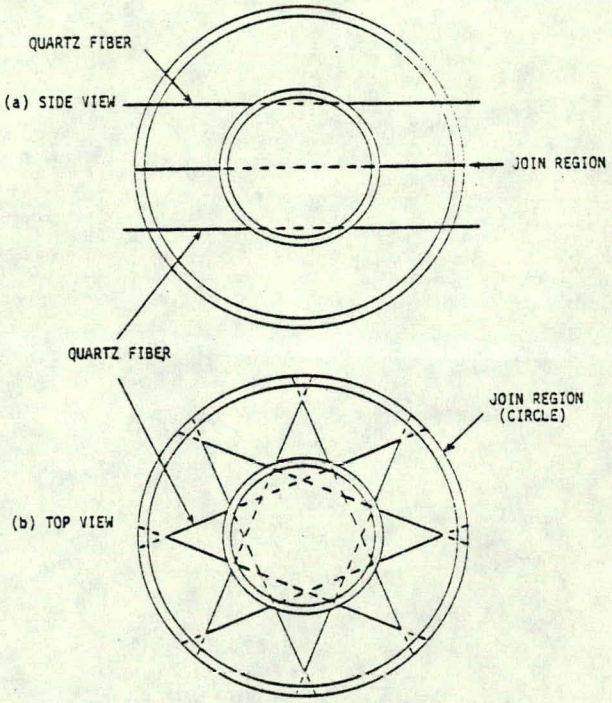

Figure 10. Suspension System for the Shell Within a Shell Pellet:
(a) Side View, (b) Top View.

Maintenance and Balance of Plant Considerations

Maintenance of the reaction chamber is based on removing the complete first wall assembly and replacing it with a new or refurbished first wall assembly in a time compatible with utility annual planned down time of about one month. The time required to perform the sequence of operations is estimated to be about 27 days and contains the following procedures: removal of components and equipment which block access; draining of the coolant; uncoupling of any connections to upper half of external spherical

shell; removal of upper outer shell from lower shell; uncoupling of inner spherical shell from its support; lifting, removing and placing inner spherical shell in a hot cell for cooldown. This process is summarized in Figure 11. Since the entire structure is radioactive, these operations are performed remotely.

The connection between the reactor and the balance of the plant is through the lithium cooling circuit which provides lithium at 369°C to the intermediate heat exchanger (liquid sodium). The total lithium flow rate required to maintain the maximum structural temperature to the allowable limit of 500°C is about 30 m^3/sec (475,000 gpm). For this conceptual design, a four loop heat transport plant was selected, with each loop having two pumps. The flow rate in each pump is thus ~4 m^3/sec (60,000 gpm), which is well within the capability of present liquid sodium pumps. The sodium hot leg temperature is 363°C, resulting in superheated steam at 358°C and with pressure of 7.24 MPa (1050 psia) which is adequate to generate electricity with 36% efficiency. The major features of the balance of plant are the heat transport, steam generator and turbine generator systems. These must be housed in containment buildings to ensure the safety of the environment against possible accident. Major buildings in the balance of plant are the Reactor Building, Hot Cell Facility Building, Steam Generator Building, Turbine Building, Pellet Factory Building, Waste Disposal Building, Control Building, Emergency Generator and Standby Generator Building and Argon Storage Building.

ICECAP Computer Code

The computer code which models the size/performance/cost of these two ICF power plants is called ICECAP, Inertial Confinement Energy, Cost and Performance Code. ICECAP was constructed such that the component models (beam driver, blanket assembly, buildings/structures/equipment, etc.) are clustered into five groups. The pellet/plant data (pellet mass, repetition rate, cavity radius, plant availability factor, etc.) is read/calculated before the first component algorithm is called and the final calculations and output provide summary data for use in trade studies. The five clusters group the component system as follows: (1) fusion support systems (drivers, pellet systems, and vacuum systems), (2) mechanical/ thermal systems (first wall, blanket, shield, primary coolant loops), (3) power supply systems (for drivers, coolant pumping, distribution, etc.), (4) turbine plant systems (turbine, steam generator, heat rejection), and (5) facilities systems (buildings, controls, remote maintenance, etc.). The pellet/ plant data is a set of internally self-consistent parameters which is used in each of the component models allowing for a single set of base assumptions in sizing and costing all subsystems. Various coding procedures are used to improve the user's ability to follow the FORTRAN as well as to identify the calculational results which are provided in the output print.

Trade Studies

Trade studies were performed using ICECAP to investigate the impact on relative cost of electricity (COE) assuming 70% availability for both driver systems and on net electrical power de-

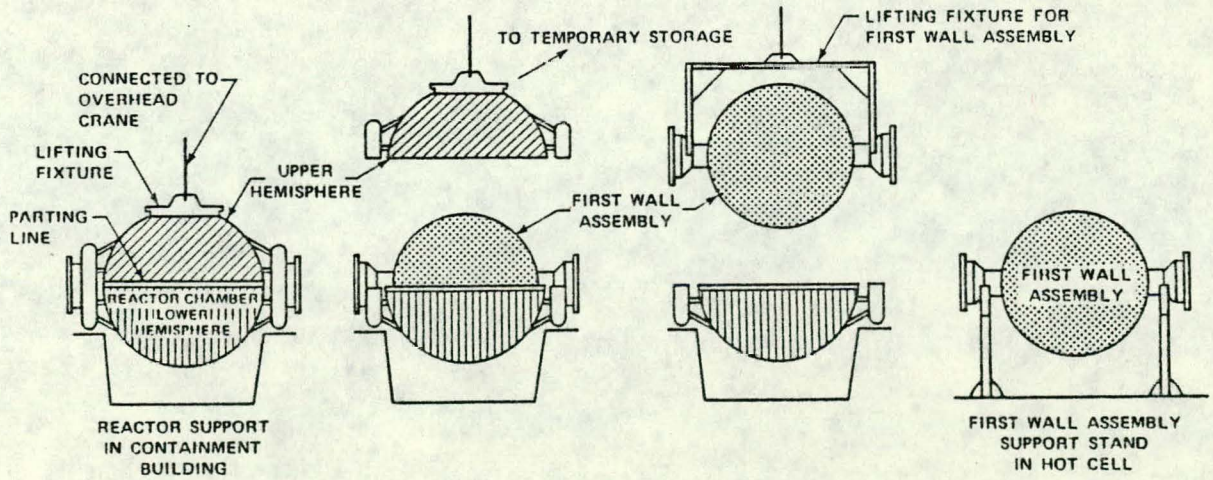

Figure 11. Sequence of Operations for the Maintenance of the First Wall

livered to the grid (P_{net}) of varying the following parameters one at a time: driver efficiency, rep rate, driver energy on target and cavity radius. Because our reference design operates at the maximum surface heat load that can be handled by our heat removal concept, parameter variations that led to heat loads greater than in the reference design were not allowed. Thus, rep rate and driver energy were varied below the reference values and cavity radius was varied above the reference value. Some interesting preliminary results for both laser and heavy ion driven reactors are listed below:

- COE drops by about 50% as rep rate increases from 5 to 10 Hz (see Figure 12).
- COE increases by only 5% as cavity radius increases from 10 to 20 m (see Figure 13).
- COE decreases by a factor of about 2 as driver energy increases from 1 to 2 MJ (see Figure 14).

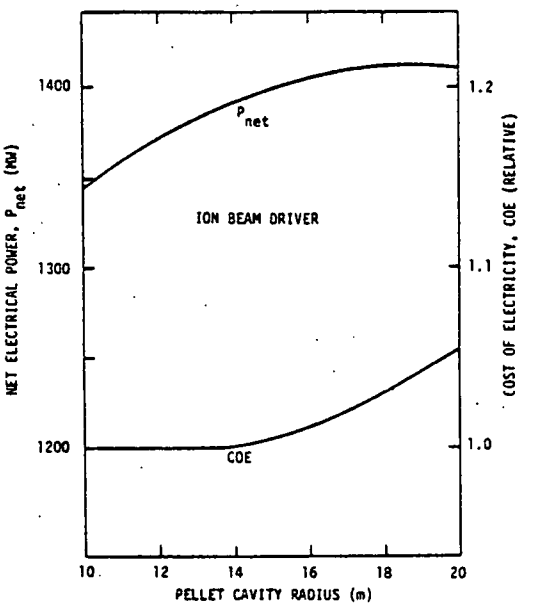

Figure 13. Cost of Electricity and Net Electrical Power Output as a Function of Pellet Cavity Radius for the Heavy-Ion Beam Driven Reactor.

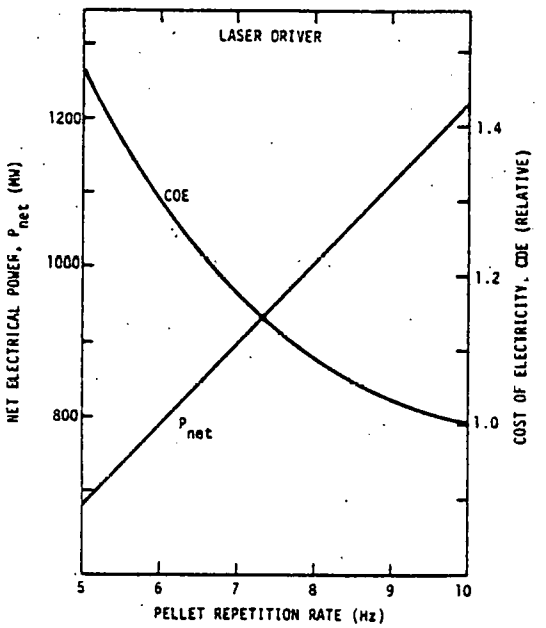

Figure 12. Cost of Electricity and Net Electrical Power Output as a Function of Pellet Repetition Rate for the Laser Driven Reactor.

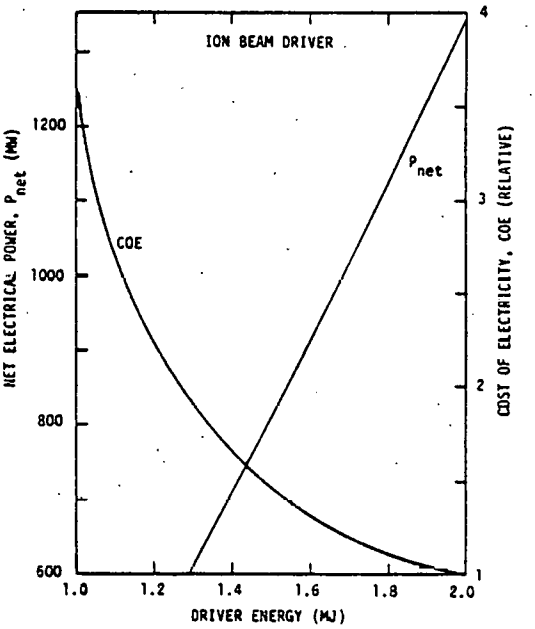

Figure 14. Cost of Electricity and Net Electrical Power Output as a Function of Driver Energy for the Heavy-Ion Beam Driven Reactor.

Conclusions

1. This study has shown that the first structural wall of an ICF reaction chamber can be protected against damage due to x-ray and ion induced temperature transients by using a thin coating of tantalum. This is a dry wall concept and is therefore compatible with cavity atmosphere requirements for all drivers. By choosing Ta as the coating material and as the heavy metal in the pellet, problems of incompatibility are removed.

2. Removal of the steady state heat load due to x-rays and ions is the limiting factor in thermal and mechanical design of the reaction chamber. Increasing cavity radius beyond our design value of 10 m will relax thermal constraints at little increase in cost of electricity but mechanical constraints may emerge at larger sizes.

3. The penalty of the low laser efficiency as compared to the heavy ion beam is about 140 MWe. Assuming 50% availability, this represents a revenue of about $30M/year. However, capital cost for the heavy ion driven reactor is greater than that for the laser driven reactor.

4. Mass production of advanced, double shell pellets can be achieved by using two novel concepts: fabrication of the spheres using a porous ceramic called MODOX, and concentrically suspending one sphere inside the other on a nest of crossed fibers.

5. Planned maintenance operations can be made compatible with time available during utility down times if the structures and maintenance machines are designed in advance for this purpose.

6. The ICECAP code provides a valuable tool for studying and comparing various ICF power plant designs and costs.

Acknowledgment

This work was performed for the Office of Fusion Energy of the U. S. Department of Energy under Contract DE-AC08-79DP40086.